Computational Materials Science 44 (2009) 895–912

Contents lists available at ScienceDirect

Computational Materials Science

journal homepage: www.elsevier.com/locate/commatsci

Expansion of plastic zone and residual stresses in the thermoplastic-matrix laminated plates ($[0°/\theta°]_2$) with a rectangular hole subjected to transverse uniformly distributed load expansion

Tamer Özben [a,*], Nurettin Arslan [b]

[a] Mechanical Engineering Department, Dicle University, 21280 Diyarbakir, Turkey
[b] Mechanical Engineering Department, Balikesir University, 10145 Balikesir, Turkey

ARTICLE INFO

Article history:
Received 2 April 2008
Accepted 18 June 2008
Available online 26 July 2008

PACS:
62.20.de
62.20.dj
62.20.dq
62.20.fg

Keywords:
Residual stress
Plastic zone
Elastic–plastic stress
Clamped and simply supported plates
Thermoplastic laminated plates
Plates with rectangular hole
Finite element method

ABSTRACT

The present paper focused on the understanding of elastic stress, residual stress and plastic zone growth in layers of stainless steel woven fiber-reinforced thermoplastic matrix composite laminated plates with rectangular hole by using the finite element method (FEM) and first-order shear deformation theory for small deformations. Moreover, the computer program was developed for small elasto-plastic stress analysis of laminated plates. The laminated plate with rectangular hole consists of four reinforced layers bonded symmetrically and antisymmetrically in $[0°/\theta°]_2$ configuration. Various applied distributed loads with different layer orientation angles and rectangular hole dimensions were used for obtaining corresponding variation of residual stresses and the expansions of the plastic regions. It was observed that the intensity of the stress components and plastic zones were the maximum near corners of the rectangular hole.

1. Introduction

The mechanical properties of the composite materials composed of base material (thermoplastic) and reinforcing fiber (woven steel fiber) are dependent on those of the constituent phases. The strength of the fiber and ductility of the matrix in the composite materials provide a new material with superior properties. These properties of the new material depend on either engineering constants or the direction of reinforcing fibers in the base material. Fiber-reinforced thermoplastic (FRT) composites are an extremely broad and versatile class of material. Woven FRT composites are now gaining popularity in manufacturing automotive and aerospace parts due to their superior reinforcing properties, ease of handling and well established textile technologies [1]. Fiber reinforced polymer composite materials offer considerable possibilities of application in aircraft, aerospace, process plants, sporting goods and military equipment on account of their high specific stiffness and specific strength. Thermoplastic composites possess the unique characteristic that they may be remolded, reprocessed and reformed, and they also offer easier storage, recycling. Composite materials are those formed by combining more than one bonded materials, each with different structural properties. An effective way is to increase the load capacity of the thermoplastic material by using reinforcement with steel or glass fibers [2]. It is quite difficult to design a machine without permitting some changes in the cross-sections of the members. These changes or discontinuities are called stress raisers, and they cause stress concentrations [3], with high stresses concentrating only in a very small region in the vicinity of the geometrical discontinuity, such as rectangular hole. The resulting plastic deformations cause strain hardening, and redistribution of localized stress concentrations to result in an increase of failure resistance of the machine component. Elastic–plastic and residual stresses are very important in failure analysis of reinforced thermoplastic-matrix laminated plates. The residual stresses acquired can be used to raise the yield points of the laminated plates. Prediction and measurement of the plastic regions and residual stresses are important in relation to production, design, and performance of composite components [4].

* Corresponding author. Tel.: +90 412 2488403; fax: +90 412 2488405.
E-mail address: tamoz@dicle.edu.tr (T. Özben).

0927-0256/$ - see front matter © 2008 Elsevier B.V. All rights reserved.
doi:10.1016/j.commatsci.2008.06.011

Elastic–plastic behavior of woven-steel-fiber-reinforced thermoplastic laminated plates under in-plane loading was investigated by Karakuzu et al. [5]. A study of enhancement of low velocity impact damage resistance of sandwich plates was carried out by Suvorov and Dvorak. In this study, interlayer reduces the strain energy release rates of interfacial cracks driven by residual stresses generated by foam core compression [6]. Portu et al. have studied the effect of residual stresses on the fracture behaviors of notched laminated composites loaded in flexural geometry [7]. Shim and Yang [8] have investigated the characterization of residual mechanical properties of woven fabric reinforced composites after low-velocity impact. It was noticed that the residual strength and stiffness of impacted laminates decreased with increasing impact damage area. Sayman has studied elastic–plastic stress analysis of symmetric aluminum metal-matrix composite laminated plates under thermal loads varying linearly. An analytical solution was performed for satisfying thermal elastic–plastic stress-strain relations and boundary conditions for small plastic deformations [9]. In a similar study, Arslan and Özben performed an elastic–plastic stress analysis in a unidirectional reinforced steel fiber thermoplastic composite cantilever beam loaded by a single force at the free end. The composite material is assumed to be hardening linearly [10]. Karakuzu et al. investigated the effect of ply number, orientation angle and bonding type on residual stress of woven steel fiber reinforced thermoplastic laminated composite plates subjected to transverse uniform load [11]. In the other study, the elasto-plastic stress analysis of thermoplastic matrix plates with rectangular hole is carried out under in-plane loading condition by Arslan [12]. There are many investigations about elastic–plastic stress analysis of fiber reinforced laminated composite plates [13–17] and inelastic behavior of composite materials [18,19].

The geometry of the square orthotropic laminated plate with rectangular hole in cartesian coordinates and boundary conditions is shown in Fig. 1. In this paper, elastic–plastic stress analysis is carried out by using FEM for thermoplastic (low density polyethylene, LDPE) matrix composite laminated plates reinforced by woven stainless steel fibers under transverse uniform loading for small deformations (Fig. 2). The laminated plates with rectangular hole are stacked in $[0°/\theta°]_2$ configurations for simply and clamped supporting type under symmetric and antisymmetric laminations. Different stacking sequences of $[0°/\theta°]_2$ ($[0°/0°]_2$, $[0°/15°]_2$, $[0°/30°]_2$, $[0°/45°]_2$) laminated composite plates are used in analysis and the results are compared with each other. Elastic, plastic, residual stresses and the expansion of the plastic zone are obtained. The loading is increased by 0.0001 MPa increments at each load step (or iteration) which is chosen as 25, 50, 75 and 100. (Fig. 3). The stress components and the spread of the plastic region are obtained for different thermoplastic materials, stacking sequences, ply orientations, rectangular hole dimensions and increasing loads in symmetric and antisymmetric laminations. Tsai–Hill theory is used as a yield criterion for anisotropic material in the solution.

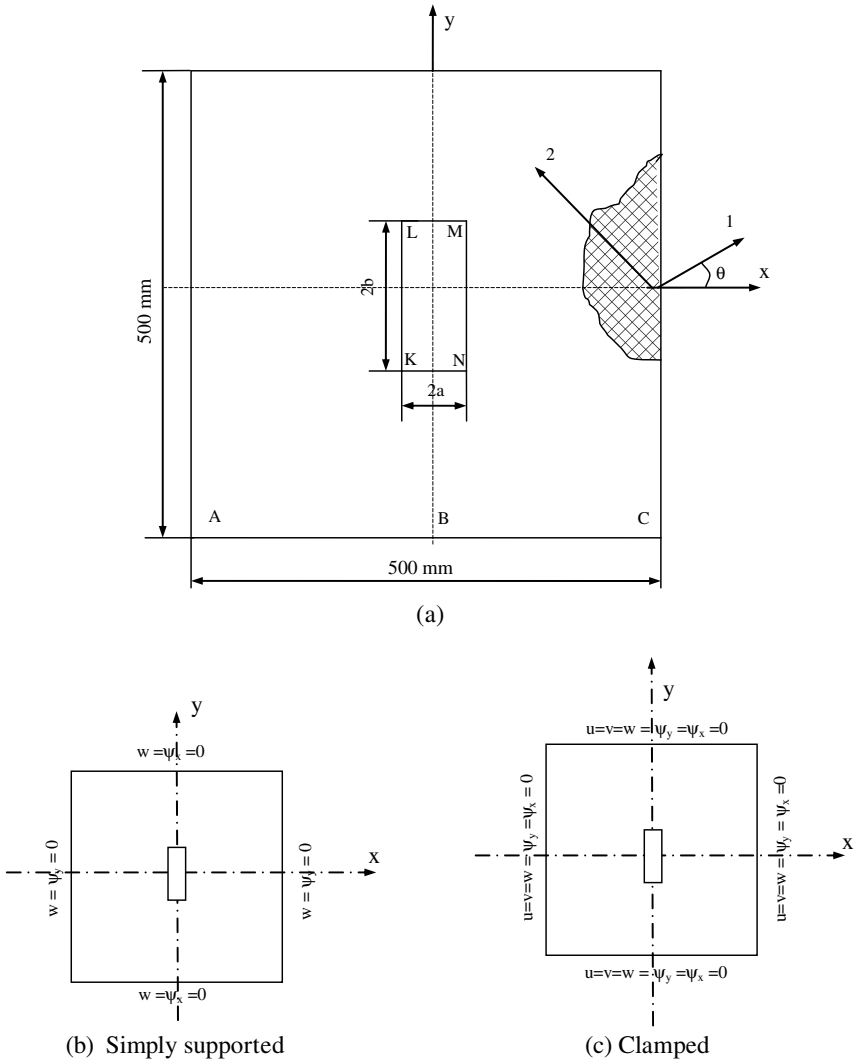

Fig. 1. Geometry (a) and boundary conditions (b and c) of the loaded plate with rectangular hole in Cartesian coordinates and simply supported-clamped supports.

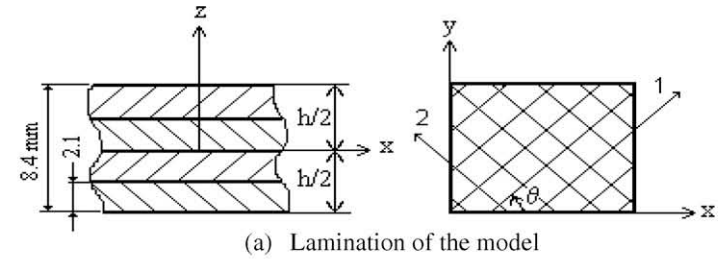

(a) Lamination of the model

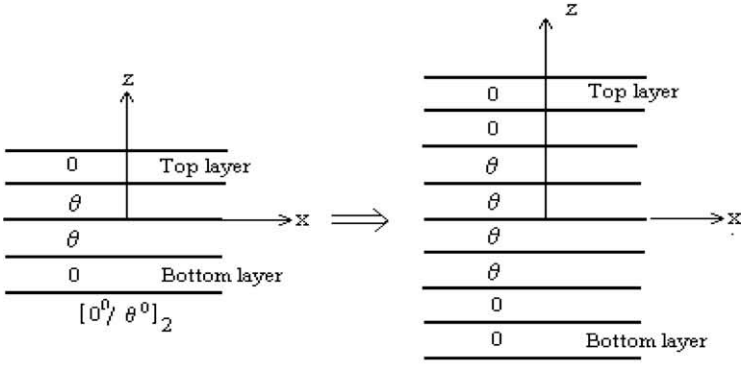

(b) A typical laminated plate divided into 8 imaginary layers.

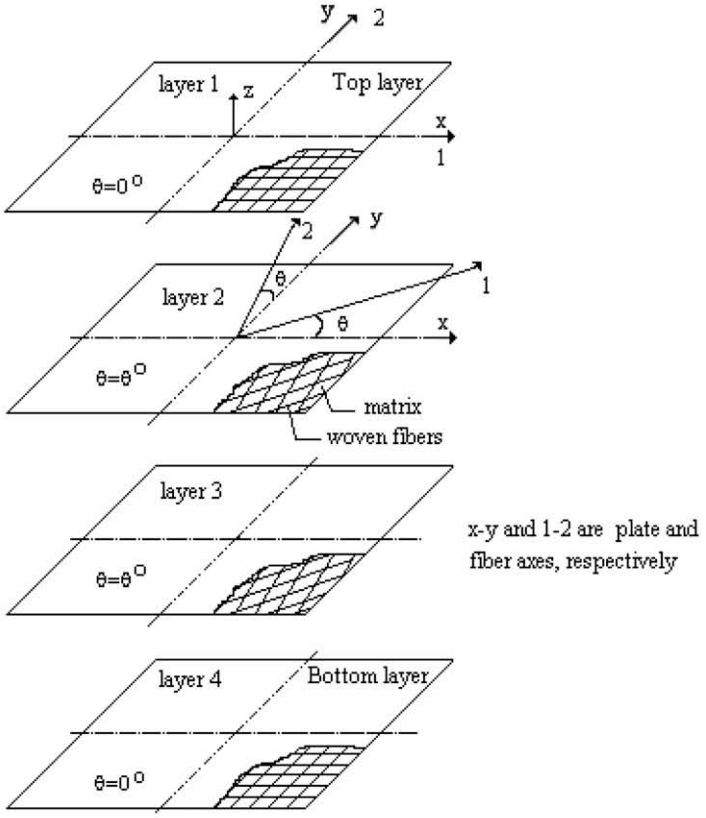

(c) $[0^0/\theta^0]_2$ orientation type of the woven cross-ply reinforced layers.

Fig. 2. A Layered section for symmetric lamination.

2. Mathematical formulation

The composite laminated plate consists of four orthotropic layers of constant thickness of 2.1 mm bonded symmetrically or antisymmetrically by heating and press load about the middle surface of the plate. Considering transverse shear deformations in the solution of the laminated plate, the relationships between stress and strains for *k*th layer of the multilayered laminate for bending and shear terms are given as, respectively [20]

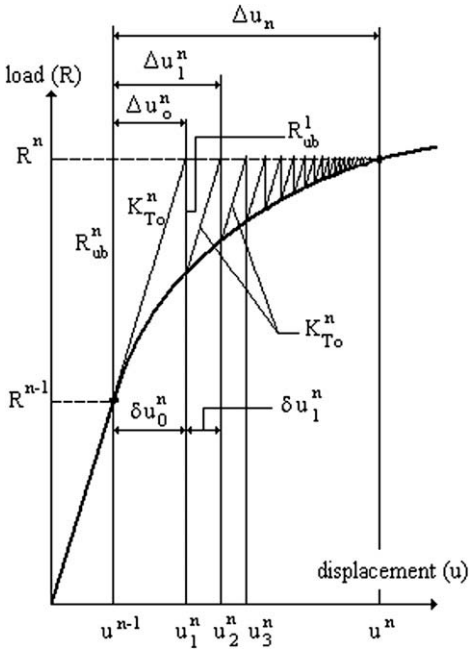

Fig. 3. Modified Newton–Raphson method ($R_{unbalanced}$=R_{ub}) [25].

$$\begin{Bmatrix}\sigma_x\\ \sigma_y\\ \tau_{xy}\end{Bmatrix}_k = \begin{bmatrix}\overline{Q}_{11}\overline{Q}_{12}\overline{Q}_{16}\\ \overline{Q}_{21}\overline{Q}_{22}\overline{Q}_{26}\\ \overline{Q}_{61}\overline{Q}_{62}\overline{Q}_{66}\end{bmatrix}_k \begin{Bmatrix}\varepsilon_x\\ \varepsilon_y\\ \gamma_{xy}\end{Bmatrix}_k, \tag{1.a}$$

$$\begin{Bmatrix}\tau_{yz}\\ \tau_{xz}\end{Bmatrix}_k = \begin{bmatrix}\overline{Q}_{44}\overline{Q}_{45}\\ \overline{Q}_{54}\overline{Q}_{55}\end{bmatrix}_k \begin{Bmatrix}\gamma_{yz}\\ \gamma_{xz}\end{Bmatrix}_k, \tag{1.b}$$

where $\overline{Q}_{ij}$ is the transformed reduced stiffness matrix and consists of orientation angle, θ, and the engineering constants of material. Each layer has a distinct fiber orientation denoted θ_k. u, v and w give the displacements of the plate in the x, y and z directions, respectively. The following assumptions are fundamental to lamination theory; the laminate consists of perfectly bonded layers (lamina), each layer is homogeneous material with known effective properties, individual layer properties can be isotropic, orthotropic or transversely isotropic, each layer is in a stage of plane stress [21]. According to the deformation theory, the first-order shear deformation theory used in this solution, normal to the middle surface remain straight and normal during deformation [2,4,20]. The midsurface of the plate is the same with x–y surface. On the basis of these assumptions, the displacement field in the plate can be expressed for small deformations as,

$$\begin{aligned} u(x,y,z) &= u_0(x,y) + z\psi_x(x,y),\\ v(x,y,z) &= v_0(x,y) - z\psi_y(x,y),\\ w(x,y) &= w_0(x,y), \end{aligned} \tag{2}$$

where u_0, v_0, and w_0 are the midsurface displacements and ψ_x and ψ_y give rotations about the normal to the y- and x-axes, respectively (Fig. 4). The bending strains change linearly through the laminated plate thickness as given below,

$$\begin{Bmatrix}\varepsilon_x\\ \varepsilon_y\\ \gamma_{xy}\end{Bmatrix} = \begin{Bmatrix}\frac{\partial u_0}{\partial x}\\ \frac{\partial v_0}{\partial y}\\ \frac{\partial u_0}{\partial y}+\frac{\partial v_0}{\partial x}\end{Bmatrix} + z\begin{Bmatrix}\frac{\partial \psi_x}{\partial x}\\ -\frac{\partial \psi_y}{\partial y}\\ \frac{\partial \psi_x}{\partial y}-\frac{\partial \psi_y}{\partial x}\end{Bmatrix}. \tag{3.a}$$

It is noted that the transverse shear strains are assumed to be constant throughout the plate thickness as [20],

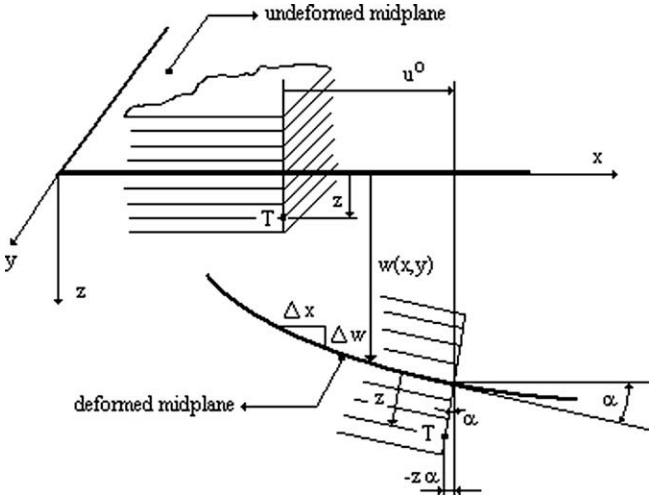

Fig. 4. Deformation of the laminated midplane [27].

$$\begin{Bmatrix}\gamma_{yz}\\ \gamma_{xz}\end{Bmatrix} = \begin{Bmatrix}\frac{\partial w}{\partial y}-\psi_y\\ \frac{\partial w}{\partial x}+\psi_x\end{Bmatrix}. \tag{3.b}$$

The total potential energy of a laminated plate under static loading is given as,

$$\Pi = U_b + U_s + V, \tag{4}$$

where U_b, and U_s are the strain energy of bending and of shear, respectively, and V presents potential energy of external forces [2,4,14]. U_b, U_s, and V are given by,

$$\begin{aligned} U_b &= \frac{1}{2}\int_{-\frac{h}{2}}^{\frac{h}{2}}\left[\int_A(\sigma_x\varepsilon_x+\sigma_y\varepsilon_y+\tau_{xy}\gamma_{xy})\mathrm{d}A\right]\mathrm{d}z,\\ U_s &= \frac{1}{2}\int_{-\frac{h}{2}}^{\frac{h}{2}}\left[\int_A(\tau_{xz}\gamma_{xz}+\tau_{yz}\gamma_{yz})\mathrm{d}A\right]\mathrm{d}z,\\ V &= -\int_A w\cdot p\cdot \mathrm{d}A - \int_{\partial R}(\overline{N}_n^b u_n^0 + \overline{N}_s^b u_s^0)\mathrm{d}s, \end{aligned} \tag{5}$$

where R is the region of a rectangular hole, and h is the total thickness of the plate, p is the transverse loading per unit area, $\overline{N}_n^b$ and $\overline{N}_s^b$ are the in-plane loads applied on the boundary ∂R. The resultant forces (N_x, N_y, N_{xy}) and moments (M_x, M_y, M_{xy}) and shear forces (Q_x, Q_y) per unit length of the cross sections of the laminated plate are obtained as given below,

$$\begin{Bmatrix}N_x, M_x\\ N_y, M_y\\ N_{xy}, M_{xy}\end{Bmatrix} = \int_{-\frac{h}{2}}^{\frac{h}{2}}\begin{Bmatrix}\sigma_x\\ \sigma_y\\ \tau_{xy}\end{Bmatrix}(1,z)\mathrm{d}z, \tag{6.a}$$

$$\begin{Bmatrix}N_{xz}\\ N_{yz}\end{Bmatrix} = \begin{Bmatrix}Q_x\\ Q_y\end{Bmatrix} = \int_{-\frac{h}{2}}^{\frac{h}{2}}\begin{Bmatrix}\tau_{xz}\\ \tau_{yz}\end{Bmatrix}\mathrm{d}z. \tag{6.b}$$

2.1. Elastic–plastic solution

In the elastic–plastic solution, strain increment are given by $\{d\varepsilon\} = \{d\varepsilon_e\} + \{d\varepsilon_p\}$, where $\{d\varepsilon_e\}$ and $\{d\varepsilon_p\}$ are the elastic and plastic components of the strain increments, respectively. The property of strain hardening increases the size of the yield points of material such as laminated composites. Thus the progression past the yield surface $d\sigma_p^*$ is given by [28,29].

$$d\sigma_p^* = \left\{\frac{\partial f}{\partial \sigma}\right\}^T\cdot\{d\sigma\} = F^T\cdot\{d\sigma\}, \tag{7}$$

where $f(\{\sigma\})$ defines the equivalent uniaxial stress σ_e(or σ^*) and, as it is obtained from the Tsai–Hill yield criterion. The multiaxial case is reduced to a uniaxial case by using the effective or equivalent stress, σ_e [1]. The elasto-plastic stress analysis is performed when the equivalent stress exceeds the yield strength of the material.

The mechanical properties consisting of yield points and plastic parameters of a layer for material produced by heating press (see Fig. 5) designed at the Firat University Mechanical Laboratory [12,28] were obtained experimentally from measured values found by using strain gages as shown in the literature [23,28] and are given in Table 1. The mechanical tests and measurements according to the relevant ASTM standards were realised in the Mechanical laboratories of Dokuz Eylul and Firat Universities by using electro-mechanical test systems (Instron and Utest, respectively) and strain indicator with data acquisition (Measurements Group-Strain indicator P-350A, Iotech DBK43A and DaqBoard/2000). There is no debonding between fibre and matrix. It is sufficient to measure longitudinal (X) and transverse (Y) tensile strengths of woven lamina; Young's moduli, E_1 and E_2; and Poisson's ratio ν_{12} by only testing longitudinal (0°) specimens, since specimens are woven. Because of the woven lamina, it is obvious that E_1, and X are equal to E_2, and Y, respectively. These properties and shear strength, S given in Table 1 had been measured in the study [4,28] by using strain gages which are bonded on the specimens in longitudinal, transverse, and 45° directions. It is assumed that the yield point, in the z direction, Z is equal to the yield point Y, in the y direction. The yield points of τ_{xz}, τ_{yz} are assumed to be equal to S which is the yield point of τ_{xy}. Because of the reinforcing steel fibres, the composite layer possesses the same yield points in tension and compressions for numerical solution [30]. Thus according to the Tsai–Hill theory,

$$\sigma_e^2 = \sigma_1^2 - \sigma_1\sigma_2 + \sigma_2^2 \left(\frac{X^2}{Y^2}\right) + (\tau_{12}^2 + \tau_{13}^2 + \tau_{23}^2) \left(\frac{X^2}{S^2}\right) = X^2, \tag{8}$$

where σ_1, σ_2,τ_{12},τ_{13} and τ_{23} are the stress components in the principal material directions. The yield function f is,

$$f = \sigma_e - X = \sigma_e - \sigma_0 = 0, \tag{9}$$

where σ_0 is the yield stress [29].

$$f(\sigma_x, \sigma_y, , \tau_{xy}, \tau_{xz}, \tau_{yz}) = [\sigma_x^2 - \sigma_x\sigma_y + \sigma_y^2 \left(\frac{X^2}{Y^2}\right) + (\tau_{xy}^2 + \tau_{xz}^2 + \tau_{yz}^2) \left(\frac{X^2}{S^2}\right)]^{1/2}, \tag{10}$$

Table 1
The mechanical properties and yield points of woven reinforced thermoplastic composite layers for different materials

Materials [4]		
E_1	(MPa)	9550
E_2	(MPa)	9550
G_{12}	(MPa)	670
ν_{12}	(MPa)	0.32
X, Axial yield value	(MPa)	18.5
Y, Transverse yield value	(MPa)	18.5
S, Shear yield value	(MPa)	8.26
K, Hardening parameter (plasticity constant)	(MPa)	99.5
n, Strain hardening exponent	(–)	0.676
V_f, Fiber volume fraction	(–)	0.07

and when the numerical value of this, the equivalent uniaxial stress σ^*, equals or exceeds X, yielding occurs. The rate of progression past the yield surface $d\sigma_p^*$ can be calculated using a plastic flow law obtained by chain differentiation of the yield function f of Eq. (11) giving [28,31]

$$F = \left\{2\sigma_x - \sigma_y, 2\sigma_y\frac{X^2}{Y^2} - \sigma_X, 2\tau_{xy}\frac{X^2}{S^2}, 2\tau_{xz}\frac{X^2}{S^2}, 2\tau_{yz}\frac{X^2}{S^2}\right\} 1/2\sigma_e. \tag{11}$$

One can write by using the elasticity matrix

$$\{d\sigma\} = D \cdot \{d\varepsilon\} - D \cdot \{d\varepsilon_p\}. \tag{12}$$

Using Eq. (8) the following equation can be obtained

$$d\sigma_p^* == F^T \cdot D \cdot \{d\varepsilon\} - F^T \cdot D \cdot \{d\varepsilon_p\}. \tag{13}$$

A hardening rule based on uniaxial behaviour is introduced [25],

$$d\sigma_p^* = H \cdot d\varepsilon_p^*, \tag{14}$$

where H is the slope of the uniaxial stress-plastic strain curve in the plastic range. Assuming also an associated flow rule for the plastic strain increments:

$$\{d\varepsilon_p\} = F \cdot d\varepsilon_p^*, \tag{15}$$

where $d\varepsilon_p^*$ corresponds to $d\sigma_p^*$ [28,29,31]. This is referred to as the Prandtl–Reuss flow rule. A symmetric tangent modulus matrix, D_T, is obtained by using (13)–(16),

$$D_T = D - \frac{D \cdot F \cdot F^T \cdot D}{H + F^T \cdot D \cdot F}. \tag{16}$$

This replaces the elastic modulus matrix, D, when $\sigma_{e_i} \geqslant \sigma_0$ in the load increment i [28,29,32,33].

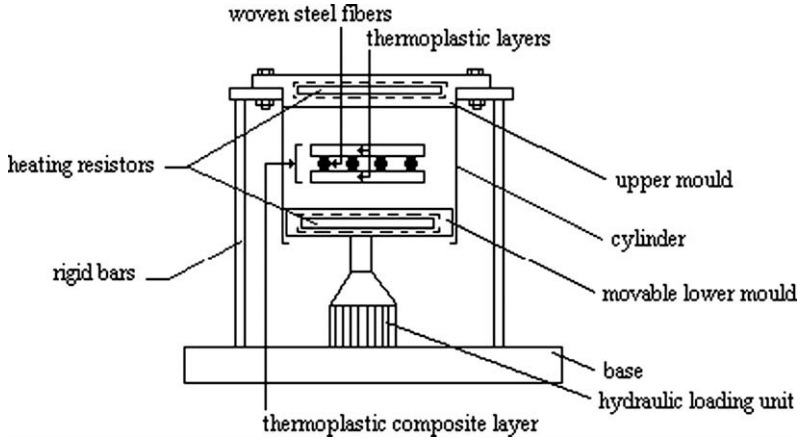

Fig. 5. Production set up of the thermoplastic composite layer by heating press.

2.2. Load stepping techniques

In this study, the used iterative solution can be derived from the Newton–Raphson method. The simplest approach to the analysis of nonlinear problems in FEM is load stepping with the total load $\{R_n\} = \sum\{\delta R_i\}$, being built up in a series of steps $i = 1 \rightarrow n$. Then the displacement solution after application of the ith load increments is obtained as

$$\{U\}_{i+1} = \{U\}_i + K_T^{-1} \cdot \{\delta R_i\}, \tag{17}$$

where K_T is tangential stiffness matrix [29]. In addition, K_T and $\{R\}$ are calculated using the displacements $\{U\}_i$, this process is repeated. This is often referred to as Euler's method. For a linear extrapolation along a tangent, Euler's formula gives

$$\varepsilon_{i+1} = \varepsilon_i + \frac{\delta\sigma}{(\mathrm{d}\sigma/\mathrm{d}\varepsilon)_i}, \tag{18}$$

where σ is stress–strain relation in plastic region, and is given by Ludwik's empirical expression as,

$$\sigma = \sigma_0 + k \cdot \varepsilon_p^n, \tag{19}$$

where σ_0 is equal to X which is the yield point in the first principal material direction, k, ε_p and n are the plasticity constant, equivalent plastic strain, and strain hardening exponent, respectively [29,31]. In addition, the empirical curves [34] for σ in Eq. (20) are given in Fig. 6. If the strain hardening exponents, n, changing from 0 to 1, have 0 and 1 values the materials are called ideal plastic and ideal elastic, respectively [35]. The mentioned material properties were attained experimentally from the load–displacement diagram.

3. Finite element analysis

In this study, a nine-node Lagrangian finite element is used to acquire the first yield point, the residual stresses, and the spread of the plastic zone of the laminated composite plates with rectangular hole for all selected materials. In this analysis, the symmetric and antisymmetric laminated plates are composed of four layers. The plates are divided into eight imaginary parts (Fig. 2) for obtaining the results more accurately [19]. The laminated plates are loaded transversely with simply supported and clamped boundary conditions shown in Fig. 1 where the middle surface of the plate coincides with the xy plane. In the FEM solution, each layer in the laminated plate having geometric and loading symmetry is automatically meshed into 64 element 288 nodes to compare with the obtained values and the literature values more accurately [1,19]. The displacement field can be expressed in the following matrix form as [22],

$$[d] = \begin{bmatrix} u_0 \\ v_0 \\ w \\ \psi_x \\ \psi_y \end{bmatrix} = \sum_{i=1}^{n} \begin{bmatrix} N_i & 0 & 0 & 0 & 0 \\ 0 & N_i & 0 & 0 & 0 \\ 0 & 0 & N_i & 0 & 0 \\ 0 & 0 & 0 & N_i & 0 \\ 0 & 0 & 0 & 0 & N_i \end{bmatrix} \begin{bmatrix} u_0 \\ v_0 \\ w \\ \psi_x \\ \psi_y \end{bmatrix}, \tag{20}$$

where N_i is the shape function at the node i and n is the total number of nodes in the FE model. The relationship between strain–displacement can be expressed in Eqs. (2) and (23), respectively, by using Eq. (3) symbolically as,

$$\{\varepsilon_{bi}\} = [B_{bi}]\{u_i\}, \tag{21}$$

$$\{\varepsilon_{si}\} = [B_{si}]\{u_i\}, \tag{22}$$

where i is the node number and $[B]$ is the transformation matrix. The final form of the element stiffness matrix of the plate element is obtained by using the minimum potential energy method of the principle of virtual displacements [19,24]. Bending and shear stiffness are obtained as,

$$[K_b] = \int_A [B_b]^T [D_b].[B_b]\mathrm{d}A,$$

$$[K_s] = \int_A [B_s]^T [D_s].[B_s]\mathrm{d}A, \tag{23}$$

where

$$[D_b] = \begin{bmatrix} A_{ij} & B_{ij} \\ B_{ij} & D_{ij} \end{bmatrix}, \quad [D_s] = \begin{bmatrix} k_1^2 A_{44} & 0 \\ 0 & k_2^2 A_{55} \end{bmatrix},$$

$$(A_{ij}, B_{ij}, D_{ij}) = \int_{-\frac{h}{2}}^{\frac{h}{2}} Q_{ij}(1, z, z^2)\mathrm{d}z \ (i = j = 1, 2, 6),$$

$$(A_{44}, A_{55}) = \int_{-\frac{h}{2}}^{\frac{h}{2}} (Q_{44}, Q_{55})\mathrm{d}z, \tag{24}$$

where D_b and D_s are the elasticity matrices of bending and shear parts of the material matrix, respectively. A_{45} is negligible in comparison with A_{44} and A_{55}. k_1 and k_2 denote the shear correction factors for rectangular cross sections and are given as $k_1^2 = k_2^2 = 5/6$ [4,27].

In this work two dimensional plate elements are used instead of 3D plate element because of the plate thickness being very small [13]. In this solution, the external forces are applied transversely and are increased incrementally. For the non-linear stress analysis, the unbalanced nodal forces and the equivalent nodal forces must be calculated for each load step [4,19]. The equivalent nodal forces at each load step can be calculated as given below:

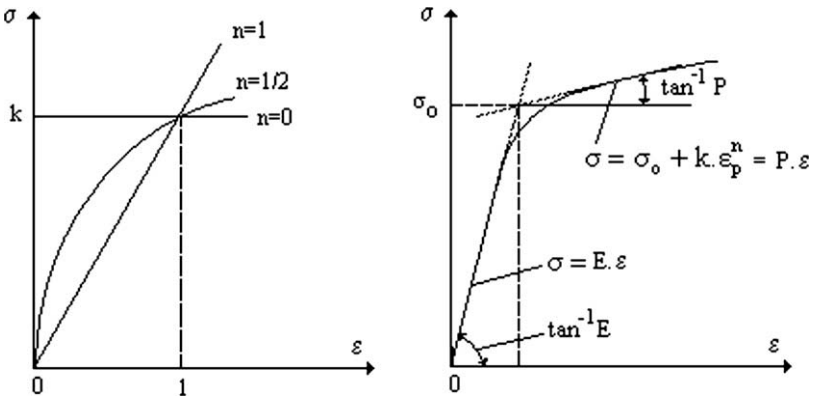

Fig. 6. Stress–strain curves (empirical curves for $\sigma = \sigma_0 + k \cdot \varepsilon_p^n = k \cdot \varepsilon^n, 0 \leqslant n \leqslant 1$) [26].

$$\{R\}_{\text{equivalent}} = \int_{vol} [B]^{\mathrm{T}} \{\sigma\} \cdot \mathrm{d}A = \int_{vol} [B_{\mathrm{b}}]^{\mathrm{T}} \{\sigma_{\mathrm{b}}\} \cdot \mathrm{d}A + \int_{vol} [B_{\mathrm{s}}]^{\mathrm{T}} \{\sigma_{\mathrm{s}}\} \cdot \mathrm{d}A. \quad (25)$$

The unbalanced nodal forces can be obtained, because the equivalent nodal forces are known. It gives

$$\{R\}_{\text{unbalanced}} = \{R\}_{\text{applied}} - \{R\}_{\text{equivalent}} = K_{\mathrm{T}} \cdot \{\delta U\}. \quad (26)$$

In the non-linear solution, the obtained unbalanced nodal forces are applied for obtaining increments by the modified Newton–Raphson method [19]. The difference between the elastic–plastic and elastic stresses gives the residual stress, RS ($=\tau^{\mathrm{I}}$). The residual stress load vector, $\{R\}_{\mathrm{I}}$ [24], is added to the total external applied load vector $\{R\}$, where Tangential stiffness matrix K_T (Fig. 5) is reevaluated if necessary by Newton–Raphson method at every iteration of every load increment under 0.001 convergence tolerance.

An elastic–plastic stresses analysis is accomplished in the clamped and simply supported laminated plates with rectangular hole under uniform transverse static loads for $[0°/\theta°]_2$ stacking sequence. The determinations of elastic–plastic solution and the plastic region distribution are completed by using symmetric and antisymmetric thermoplastic laminated plates made of four layers. The transverse load was increased to 0.0001 MPa at each load step from the yield point of the plate of different orientation angles and different supports cases.

The load steps were selected as 25, 50, 75 and 100 for clamped and simply supported cases. The difference between the plastic and elastic stresses provides the residual stress. The uniform transverse forces at the yield points of both cases are shown in Table 2. It is seen from this table that the yield points of the symmetric stacked plates are lower than those of antisymmetric stacked plates at $[0°/30°]_2$, $[0°/45°]_2$, $[0°/60°]_2$ stacking sequence for simply supported case. The appropriate values for $[0°/0°]2$, $[0°/15°]_2$, $[0°/$

Table 2
The uniform transverse force at the yield points of the simply supported and clamped laminated plates for $[0°/\theta°]$ stacking sequence (in MPa) ($a \times b = 12.5 \times 25$ in mm)[a]

Stacking sequence	$[0°/0°]_2$	$[0°/15°]_2$	$[0°/30°]_2$	$[0°/45°]_2$	$[0°/60°]_2$	$[0°/75°]_2$	$[0°/90°]_2$
Simply supported							
S	0.00849	0.00859	0.00889	0.00890	0.00889	0.00859	0.00849
AS	0.00849	0.00859	0.00919	0.00979	0.00919	0.00859	0.00849
Clamped							
S	0.02089	0.0209	0.02099	0.02099	0.02099	0.0209	0.0209
AS	0.02089	0.0203	0.01990	0.02050	0.01990	0.0203	0.0209

[a] S, AS: symmetric and antisymmetric lamination, respectively.

Table 3
Maximum plastic, elastic and residual stress components in the upper and lower layers of antisymmetric simply supported laminated plates ($[0°/45°]_2$) for 25–100 iterations (load steps)

Loads steps	Layers		σ_x (MPa)	σ_y (MPa)	τ_{xy} (MPa)	τ_{yz} (MPa)	τ_{xz}(MPa)
Plastic stresses							
25	U[a]	0°	21.340	17.086	0.414	0.149	−0.147
	L[a]	45°	−18.990	−16.454	0.275	−0.250	−0.045
50	U	0°	21.597	21.128	1.246	−0.191	0.247
	L	45°	−20.477	−18.318	0.252	−0.471	−0.062
75	U	0°	23.371	21.384	3.657	0.272	0.175
	L	45°	−21.871	−19.477	0.398	−0.381	−0.061
100	U	0°	26.396	23.575	−4.548	0.303	−0.136
	L	45°	−24.323	−20.012	0.541	−0.281	−0.021
			σ_x	σ_y	τ_{xy}	τ_{yz}	τ_{xz}
Elastic stresses							
25	U	0°	23.132	17.127	−0.082	0.252	0.043
	L	45°	−19.002	−17.120	0.293	0.252	0.043
50	U	0°	32.021	24.558	−0.126	0.485	0.061
	L	45°	−25.589	−23.635	0.437	−0.485	−0.056
75	U	0°	37.397	28.681	−0.147	0.567	0.071
	L	45°	−29.885	−27.603	0.510	−0.567	−0.066
100	U	0°	42.580	32.656	−0.168	0.645	0.081
	L	45°	−34.027	−31.429	0.581	−0.646	−0.075
			RS_{xx}	RS_{yy}	RS_{xy}	RS_{yz}	RS_{xz}
Residual stresses							
25	U	0°	−1.810	−0.764	0.002	−0.016	0.001
	L	45°	1.820	1.788	0.963	−0.015	0.001
50	U	0°	−10.771	−6.057	−0.003	−0.156	0.013
	L	45°	8.066	7.921	2.943	−0.012	0.041
75	U	0°	−16.125	−9.272	−0.010	0.249	−0.005
	L	45°	11.962	11.931	4.185	−0.055	0.086
100	U	0°	−21.262	−11.480	−0.076	0.327	0.082
	L	45°	15.886	15.656	−5.419	0.306	−0.717

[a] U, L: upper and lower layers, respectively.

Table 4
Maximum plastic, elastic and residual stress components in the upper and lower layers of antisymmetric clamped laminated plates ([0°/45°]) for 25–100 iterations (load steps)

Loads steps	Layers		σ_x (MPa)	σ_y (MPa)	τ_{xy} (MPa)	τ_{yz} (MPa)	τ_{xz} (MPa)
Plastic stresses							
25	U[a]	0°	21.340	17.086	0.414	0.149	−0.147
	L[a]	45°	−18.990	−16.454	0.275	−0.250	−0.045
50	U	0°	21.350	19.072	−0.487	0.163	0.158
	L	45°	−19.759	−16.835	0.284	0.274	0.054
75	U	0°	21.418	20.319	1.019	0.063	−0.199
	L	45°	−20.120	−16.770	0.314	0.300	0.052
100	U	0°	21.568	21.167	1.179	0.096	−0.208
	L	45°	−20.497	−18.010	0.273	0.334	0.063
			σ_x	σ_y	τ_{xy}	τ_{yz}	τ_{xz}
Elastic stresses							
25	U	0°	23.132	17.127	−0.082	0.252	0.043
	L	45°	−19.002	−17.120	0.293	0.252	0.043
50	U	0°	25.635	18.981	−0.091	0.279	0.048
	L	45°	−21.058	−18.654	0.325	0.279	0.048
75	U	0°	27.901	20.834	−0.488	0.177	0.185
	L	45°	−23.115	−20.826	0.356	0.307	0.053
100	U	0°	30.642	22.688	−0.109	−0.334	−0.058
	L	45°	−25.171	−22.679	0.388	0.334	0.058
			RS_{xx}	RS_{yy}	RS_{xy}	RS_{yz}	RS_{xz}
Residual stresses							
25	U	0°	−1.810	−0.764	0.002	−0.016	0.001
	L	45°	1.820	1.789	0.963	−0.015	0.001
50	U	0°	−4.318	−1.883	0.000	−0.042	0.006
	L	45°	3.594	3.506	1.788	0.029	0.001
75	U	0°	−6.825	−3.161	−0.004	−0.067	−0.002
	L	45°	5.412	5.315	2.521	0.020	−0.002
100	U	0°	−9.327	−4.509	−0.003	−0.090	0.013
	L	45°	7.261	7.124	−3.219	−0.034	−0.005

[a] U, L: upper and lower layers, respectively.

Table 5
Maximum elastic and residual stresses components at the corner of the rectangular hole (point K in Fig. 1) for all layers[a] in clamped and simply supported laminated plates ($[0°/45°]_2$) for 100 load steps

	Elastic stresses (MPa)					Residual stresses (MPa)				
	σ_x	σ_y	τ_{xy}	τ_{yz}	τ_{xz}	RS_{xx}	RS_{yy}	RS_{xy}	RS_{yz}	RS_{xz}
(a) Symmetric clamped laminated plates										
1 (0°)	28,956	22,504	−1,828	0,806	0,301	−8,675	−4,616	−0,443	−0,256	−0,177
2 (0°)	20,683	16,074	−1,306	0,806	0,301	−0,986	0,687	−0,357	−0,194	−0,183
3 (45°)	11,283	10,771	−4,23	0,806	0,301	1,779	1,866	−1,218	−0,227	−0,183
4 (45°)	3,761	3,59	−1,41	0,806	0,301	0,593	0,622	−0,406	−0,227	−0,183
5 (45°)	−3,761	−3,59	1,41	0,806	0,301	−0,593	−0,622	0,406	−0,227	−0,183
6 (45°)	−11,283	−10,771	4,23	0,806	0,301	−1,779	−1,866	1,218	−0,227	−0,183
7 (0°)	−20,683	−16,074	1,306	0,806	0,301	0,986	−0,687	0,357	−0,194	−0,183
8 (0)	−28,956	−22,504	1,828	0,806	0,301	8,675	4,616	0,443	−0,256	−0,177
(b) Antisymmetric clamped laminated plates										
1 (0°)	27,473	21,711	−1,803	0,526	0,008	−6,861	−3,63	−0,669	−0,135	−0,006
2 (0°)	19,686	15,797	−1,319	0,526	0,008	0,091	1,035	−0,479	0,017	−0,006
3 (45°)	11,078	10,705	−4,505	0,526	0,008	1,938	1,897	−1,228	0,11	−0,006
4 (45°)	4,054	4,028	−1,891	0,526	0,008	−0,623	−0,682	0,263	0,11	−0,006
5 (0°)	−3,676	−1,943	0,134	0,526	0,008	−3,017	−3,43	0,325	0,11	−0,006
6 (0°)	−11,463	−7,856	0,618	0,526	0,008	−5,54	−6,049	0,601	0,11	−0,006
7 (45°)	−17,017	−16,002	5,951	0,526	0,008	0,763	0,651	−0,39	0,018	−0,002
8 (45°)	−24,041	−22,679	8,565	0,526	0,008	7,261	7,124	−3,219	−0,034	−0,005
(c) Antisymmetric simply supported laminated plates										
1 (0°)	39,289	31,378	−2,388	0,284	−0,29	−12,893	−7,994	−2,16	0,019	0,154
2 (0°)	28,338	22,989	−1,76	0,284	−0,29	−5,769	−3,164	−1,586	0,049	0,139
3 (45°)	16,251	15,735	−6,111	0,284	−0,29	−0,289	−0,596	0,318	0,159	0,115
4 (45°)	6,344	6,302	−2,721	0,284	−0,29	−0,155	−0,35	−0,167	0,303	0,143
5 (0°)	−4,516	−2,178	0,124	0,284	−0,29	−8,624	−9,095	0,883	0,303	0,143
6 (0°)	−15,467	−10,567	0,752	0,284	−0,29	−5,003	−7,483	1,695	0,093	0,135
7 (45°)	−23,378	−21,996	7,452	0,284	−0,29	6,274	6,401	−2,099	0,105	0,132
8 (45°)	−33,285	−31,429	10,842	0,284	−0,29	15,429	15,655	−5,353	0,08	0,145

[a] 1,8: upper and lower surfaces, respectively.

Table 6
Maximum plastic, elastic and residual stress components in the upper and lower layers clamped laminated plates $[0°/\theta°]$ for p = 0.0219 MPa constant load

	Elastic stresses (MPa)					Residual stresses (MPa)				
	σ_x	σ_x	τ_{xy}	τ_{yz}	τ_{xz}	RS_{xx}	RS_{yy}	RS_{xy}	RS_{yz}	RS_{xz}
(a) Maximum stresses at the upper for symmetric laminated plates										
$(0°/0°)_2$	23.166	17.538	−0.071	0.417	0.037	−6.416	−3.871	0.015	0.095	−0.046
$(0°/15°)_2$	22.548	16.925	−0.083	0.390	0.028	−6.061	−3.623	−0.014	−0.094	−0.053
$(0°/30°)_2$	22.516	16.812	−0.081	0.363	0.029	−5.236	−3.043	−0.009	−0.077	−0.053
$(0°/45°)_2$	22.491	16.840	−0.066	0.352	0.036	−4.773	−2.699	−0.006	−0.064	−0.043
$(0°/60°)_2$	22.499	16.926	−0.052	0.367	0.044	−5.236	−3.043	0.009	0.077	−0.053
$(0°/75°)_2$	22.530	17.043	−0.054	0.394	0.044	−6.061	−3.623	0.014	−0.094	0.053
$(0°/90°)_2$	22.554	17.074	−0.069	0.406	0.036	−6.416	−3.871	−0.015	−0.095	−0.046
(b) Maximum stresses at the lower for symmetric laminated plates										
$(0°/0°)_2$	−23.166	−17.538	0.071	0.417	0.037	6.416	3.871	−0.015	0.095	−0.046
$(0°/15°)_2$	−22.548	−16.925	0.083	0.390	0.028	6.061	3.623	0.014	−0.094	−0.053
$(0°/30°)_2$	−22.516	−16.812	0.081	0.363	.0029	5.236	3.043	0.009	−0.077	−0.053
$(0°/45°)_2$	−22.491	−16.840	0.066	0.352	0.036	4.773	2.699	0.006	−0.064	−0.043
$(0°/60°)_2$	−22.499	−16.926	0.052	0.367	0.044	5.236	3.043	−0.009	0.077	−0.053
$(0°/75°)_2$	−22.530	−17.043	0.054	0.394	0.044	6.061	3.623	−0.014	0.094	−0.053
$(0°/90°)_2$	−22.554	−17.074	0.069	0.406	0.036	6.416	3.871	0.015	−0.095	−0.046
(c) Maximum stresses at the upper for antisymmetric laminated plates										
$(0°/0°)_2$	23.166	17.538	−0.071	0.417	0.037	−6.416	−3.871	0.015	0.095	−0.046
$(0°/15°)_2$	22.428	16.828	0.013	0.351	0.006	−5.256	−3.254	−0.014	−0.089	−0.043
$(0°/30°)_2$	22.229	16.491	−0.024	0.278	0.014	−3.166	−1.840	0.018	0.007	0.008
$(0°/45°)_2$	22.130	16.386	−0.079	0.241	0.042	−2.306	−1.284	0.006	−0.035	−0.002
$(0°/60°)_2$	22.233	16.572	0.665	−0.060	−0.154	−3.293	−1.859	−0.006	0.016	−0.024
$(0°/75°)_2$	22.490	16.895	0.658	−0.023	−0.115	−5.260	−3.255	0.013	−0.089	0.043
$(0°/90°)_2$	22.554	17.074	−0.069	−0.406	−0.036	−6.416	−3.871	0.015	0.095	−0.046
(d) Maximum stresses at the lower for antisymmetric laminated plates										
$(0°/0°)_2$	−23.166	−17.538	0.071	0.417	0.037	6.416	3.871	−0.015	0.095	−0.046
$(0°/15°)_2$	−21.997	−18.979	−3.357	−0.474	0.192	5.963	3.575	0.710	0.052	−0.006
$(0°/30°)_2$	−19.616	−18.754	−4.096	0.125	0.226	3.665	2.426	0.994	0.004	0.021
$(0°/45°)_2$	−18.179	−16.379	0.280	0.241	0.042	2.046	1.919	−0.658	−0.006	0.012
$(0°/60°)_2$	−20.125	−18.754	5.758	0.353	0.057	3.665	2.427	−0.994	−0.004	0.021
$(0°/75°)_2$	−22.031	−18.796	3.379	−0.020	0.026	5.963	3.090	−0.710	−0.052	−0.006
$(0°/90°)_2$	−22.554	−17.074	0.069	0.406	0.036	6.418	3.869	−0.016	−0.095	0.046

Table 7
Maximum elastic and residual stress components in the upper and lower layers simply supported laminated plates ($[0°/\theta°]$) for p = 0.01079 MPa constant load

Layers	Elastic stresses (MPa)					Residual stresses (MPa)				
	σ_x	σ_x	τ_{xy}	τ_{yz}	τ_{xz}	RS_{xx}	RS_{yy}	RS_{xy}	RS_{yz}	RS_{xz}
(a) Maximum stresses at the upper for symmetric laminated plates										
$(0°/0°)_2$	27.324	21.370	0.788	0.237	−0.179	−6.416	−3.871	0.015	0.095	−0.046
$(0°/15°)_2$	26.926	20.457	−0.103	0.599	0.034	−6.061	−3.623	−0.014	−0.094	−0.053
$(0°/30°)_2$	26.328	20.320	−0.098	0.553	0.034	−5.236	−3.043	−0.009	−0.077	−0.053
$(0°/45°)_2$	26.027	20.062	−0.080	0.534	0.044	−4.773	−2.699	−0.006	−0.064	−0.043
$(0°/60°)_2$	26.356	20.435	0.746	0.178	−0.176	−5.236	−3.043	0.009	0.077	−0.053
$(0°/75°)_2$	27.004	20.529	0.779	0.199	−0.170	−6.061	−3.623	0.014	−0.094	0.053
$(0°/90°)_2$	27.234	21.370	0.788	0.237	−0.179	−6.416	−3.871	−0.015	−0.095	−0.046
(b) Maximum stresses at the lower for symmetric laminated plates										
$(0°/0°)_2$	−27.234	−21.370	−0.788	0.237	−0.179	6.416	3.871	−0.015	0.095	−0.046
$(0°/15°)_2$	−26.926	−20.347	0.473	0.365	0.096	6.061	3.623	0.014	−0.094	−0.053
$(0°/30°)_2$	−26.328	−19.824	0.455	0.340	0.106	5.236	3.043	0.009	−0.077	−0.053
$(0°/45°)_2$	−26.027	−20.016	0.100	0.437	0.023	4.773	2.699	0.006	−0.064	−0.043
$(0°/60°)_2$	−26.356	−19.968	−0.746	0.178	−0.176	5.236	3.043	−0.009	0.077	−0.053
$(0°/75°)_2$	−27.004	−20.363	0.098	0.480	0.038	6.061	3.623	−0.014	−0.094	0.053
$(0°/90°)_2$	−27.234	−21.370	−0.788	0.237	−0.179	6.416	3.871	0.015	−0.095	−0.046
(c) Maximum stresses at the upper for antisymmetric laminated plates										
$(0°/0°)_2$	27.324	21.370	0.788	0.237	−0.179	−6.416	−3.871	0.015	0.095	−0.046
$(0°/15°)_2$	26.237	19.873	−0.005	0.531	0.004	−5.256	−3.254	−0.014	−0.089	−0.043
$(0°/30°)_2$	24.460	18.363	−0.043	0.409	0.013	−3.166	−1.840	0.018	0.007	0.008
$(0°/45°)_2$	23.634	18.126	−0.093	0.358	0.045	−2.306	−1.284	0.006	−0.035	−0.002
$(0°/60°)_2$	24.515	18.938	0.688	0.050	−0.176	−3.293	−1.859	−0.006	0.016	−0.024
$(0°/75°)_2$	26.399	19.906	0.723	0.110	−0.152	−5.260	−3.255	0.013	−0.089	0.043
$(0°/90°)_2$	27.234	21.370	0.788	0.237	−0.179	−6.416	−3.871	0.015	0.095	−0.046
(d) Maximum stresses at the lower for antisymmetric laminated plates										
$(0°/0°)_2$	−27.234	−21.370	−0.788	0.237	−0.179	6.416	3.871	−0.015	0.095	−0.046
$(0°/15°)_2$	−26.045	−22.392	−3.703	−0.244	−0.019	5.963	3.575	0.710	0.052	−0.006
$(0°/30°)_2$	−22.037	−20.567	−5.846	−0.125	−0.129	3.665	2.426	0.994	0.004	0.021
$(0°/45°)_2$	−18.886	−17.444	0.247	0.358	0.045	2.046	1.919	−0.658	−0.006	0.012
$(0°/60°)_2$	−22.037	−20.567	5.846	0.125	−0.129	3.665	2.427	−0.994	−0.004	0.021
$(0°/75°)_2$	−26.045	−22.392	3.703	0.244	−0.019	5.963	3.090	−0.710	−0.052	−0.006
$(0°/90°)_2$	−27.234	−21.370	−0.788	0.237	−0.179	6.418	3.869	−0.016	−0.095	0.046

$75°]_2$, $[0°/90°]_2$ stacking sequence are the same for simply supported case. However, the yield points of the symmetric stacked plates are higher than those of antisymmetric stacked plates at $[0°/15°]_2$, $[0°/30°]_2$, $[0°/45°]_2$, $[0°/60°]$ and $[0°/75°]_2$ stacking sequence for clamped case. The relevant values for $[0°/0°]_2$ and $[0°/90°]_2$ stacking sequence are the same for clamped case. The yield

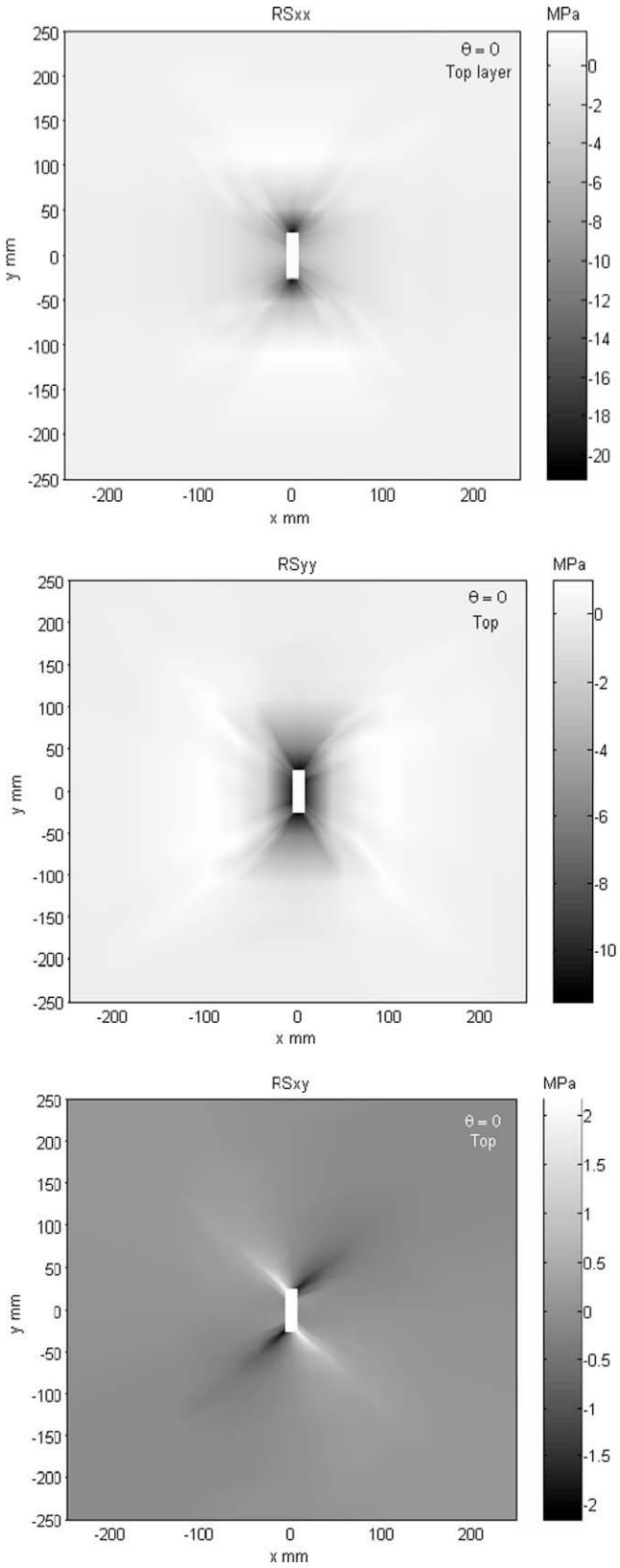

Fig. 7. Mapping of residual stresses components on the top layer ($\theta = 0°$) for antisymmetric simply supported laminated plate ($[0°/45°]_2$ and 100 load steps.

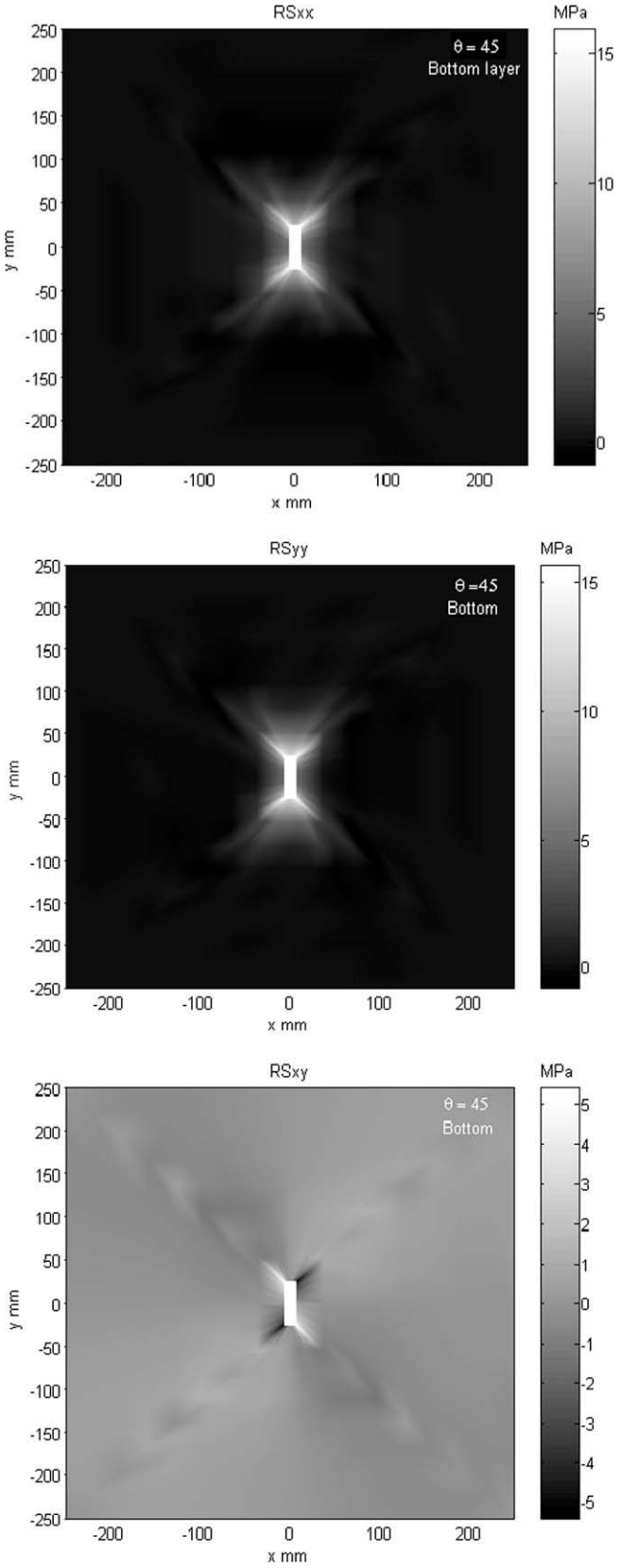

Fig. 8. Mapping of residual stresses components on the bottom layer ($\theta = 45°$) for antisymmetric simply supported laminated plate ($[0°/45°]_2$) and 100 load steps.

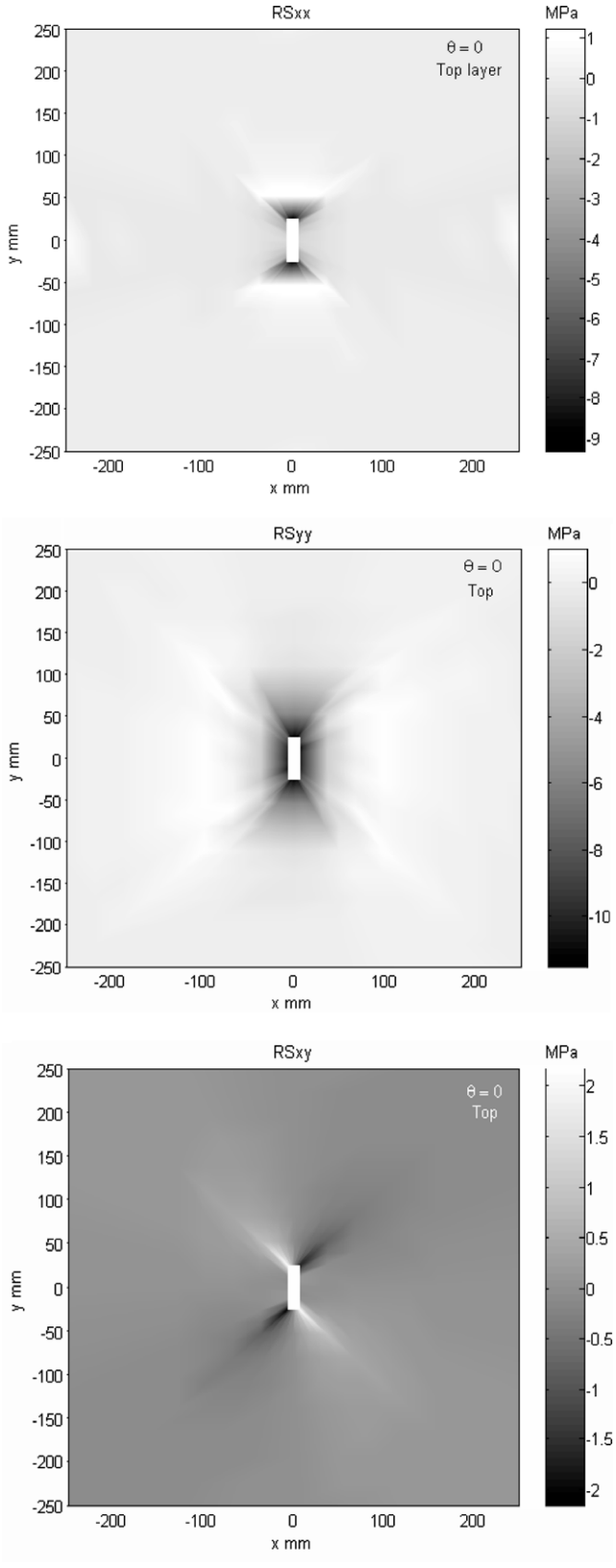

Fig. 9. Mapping of residual stresses components on the top layer ($\theta = 0°$) for antisymmetric clamped laminated plate ($[0°/45°]_2$) and 100 load steps.

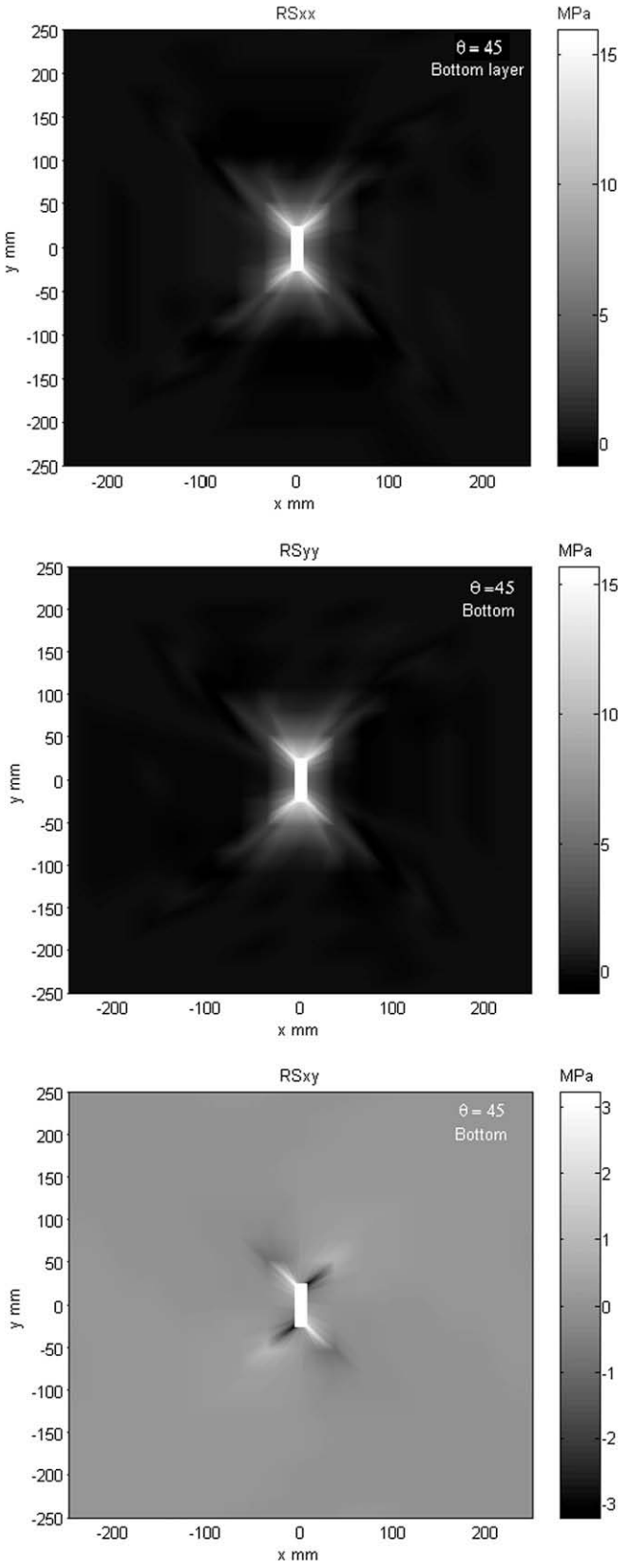

Fig. 10. Mapping of residual stresses components on the bottom layer ($\theta = 45°$) for antisymmetric clamped laminated plate ($[0°/45°]_2$) and 100 load steps.

points of the symmetric and the antisymmetric laminated clamped plates are, it is observed, higher than those of simply supported plates.

The concentration of stress components and the expansion of the plastic zone at the upper and lower surfaces of symmetric oriented laminates for both clamped and simply supported boundary

cases are the same, thus they can be given in the figures only for first (top) layers. Moreover they are the same in symmetric and antisymmetric laminated plates for all the stacking sequence of $[0°/0°]_2$ and $[0°/90°]_2$, since the plates are reinforced by woven fibers.

The maximum plastic, elastic and residual stress components at the upper and lower layers of antisymmetric simply and clamped supported for 25–100 load steps and $[0°/45°]_2$ stacking sequence, the results are shown in Tables 3 and 4 in which variations of the plastic, elastic stress components ($\sigma_{xx} = S_{xx}$, $\sigma_{yy} = S_{yy}$, $\tau_{xy} = S_{xy}$, $\tau_{yz} = S_{yz}$, $\tau_{xz} = S_{xz}$) and residual stresses components (RS_{xx}, RS_{yy}, RS_{xy}, RS_{yz}, RS_{xz}) with respect to load steps are also provided. It is noticed that stress and residual stress values increase with increasing load steps these conclusion are predicted as well. Furthermore, a similar behavior can be observed clamped plates. This event can also be obtained for the laminated plate with square hole [4].

Table 5 provides the maximum elastic and residual stress components at the corner of the rectangular hole (point *K*) for all layers in clamped and simply supported laminated plates $[0°/45°]_2$. The layers are stacked symmetrically and antisymmetrically and the load step is 100. It is observed that the stress values at the upper and lower layers are higher than those at inner layers for either symmetric or antisymmetric lamination due to the loading condition. The same situation can be noticed in both clamped and simply supported laminated plates. The smallest elastic and residual stress values are obtained at the layers which are adjacent to the

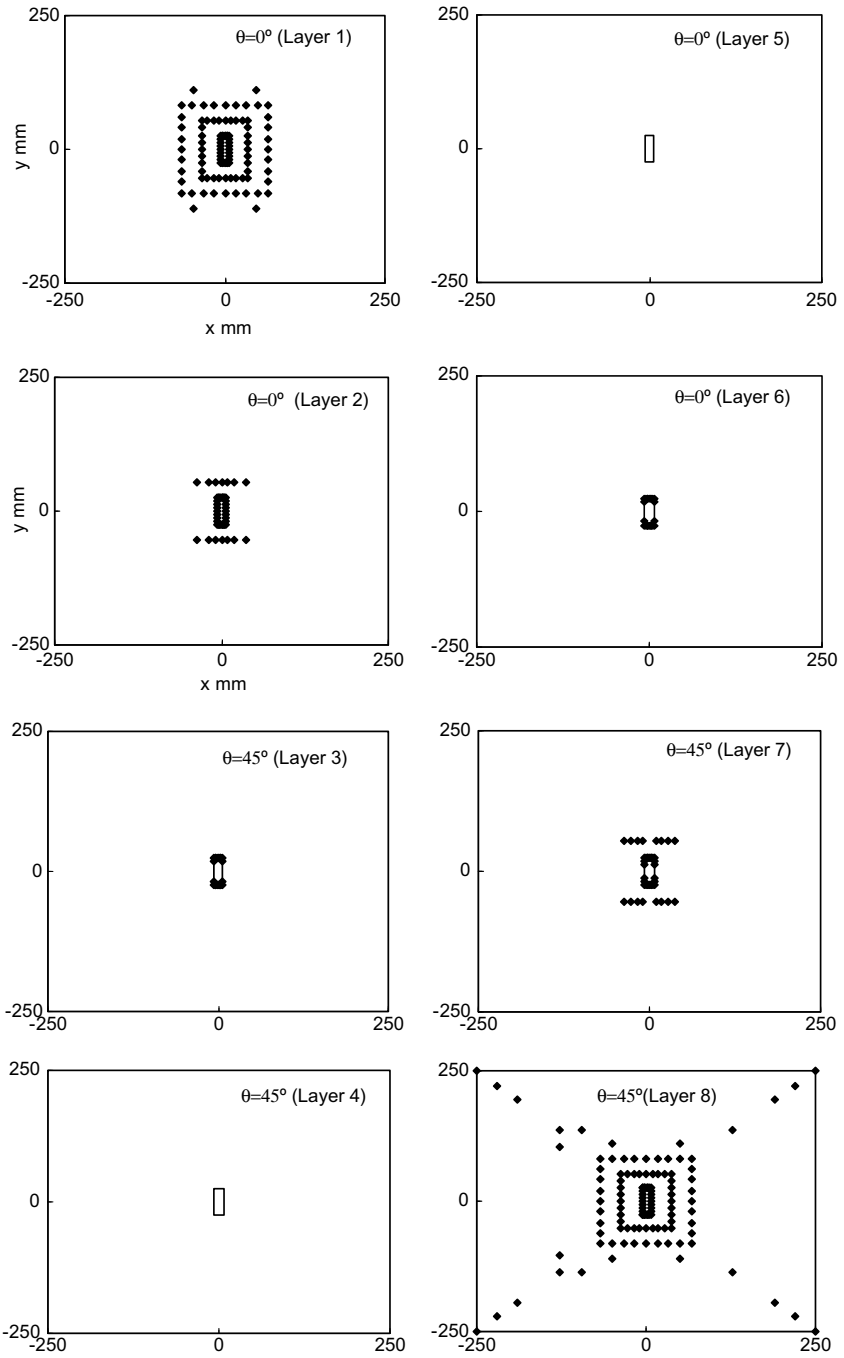

Fig. 11. Nodes in plastic region at each layer for antisymmetric ($[0°/45°]_2$) simply supported laminated plates and 100 load steps.

midplane in either clamped or simply supported plates for symmetric and antisymmetric lamination, as expected. In addition, elastic and residual stress values at layers having the same distance from the midplane are absolutely equal for symmetric lamination. As determined from Table 5, the elastic and residual stress values for the simply supported case are higher than those for clamped case. Furthermore, the stress components for the symmetric cases are higher than those for antisymmetric cases (RS_{xx} = 8.675 and 7.261 MPa in 8th layers for symmetric and antisymmetric lamination, respectively). The results were recognized with other studies [4,14].

The maximum stresses in clamped case for different stacking sequence ($[0°/\theta°]_2$) and symmetric and antisymmetric lamination at p = 0.0219 MPa constant load are presented in Table 6. The maximum stress values at $[0°/45°]_2$ stacking sequence are smaller than those at $[0°/\theta°]_2$ (θ = 0°, 15°, 30°, 60°, 75° and 90°) for either symmetric or antisymmetric lamination. The stress values at θ = 0° and 90° layers (upper and lower surfaces) are absolutely same

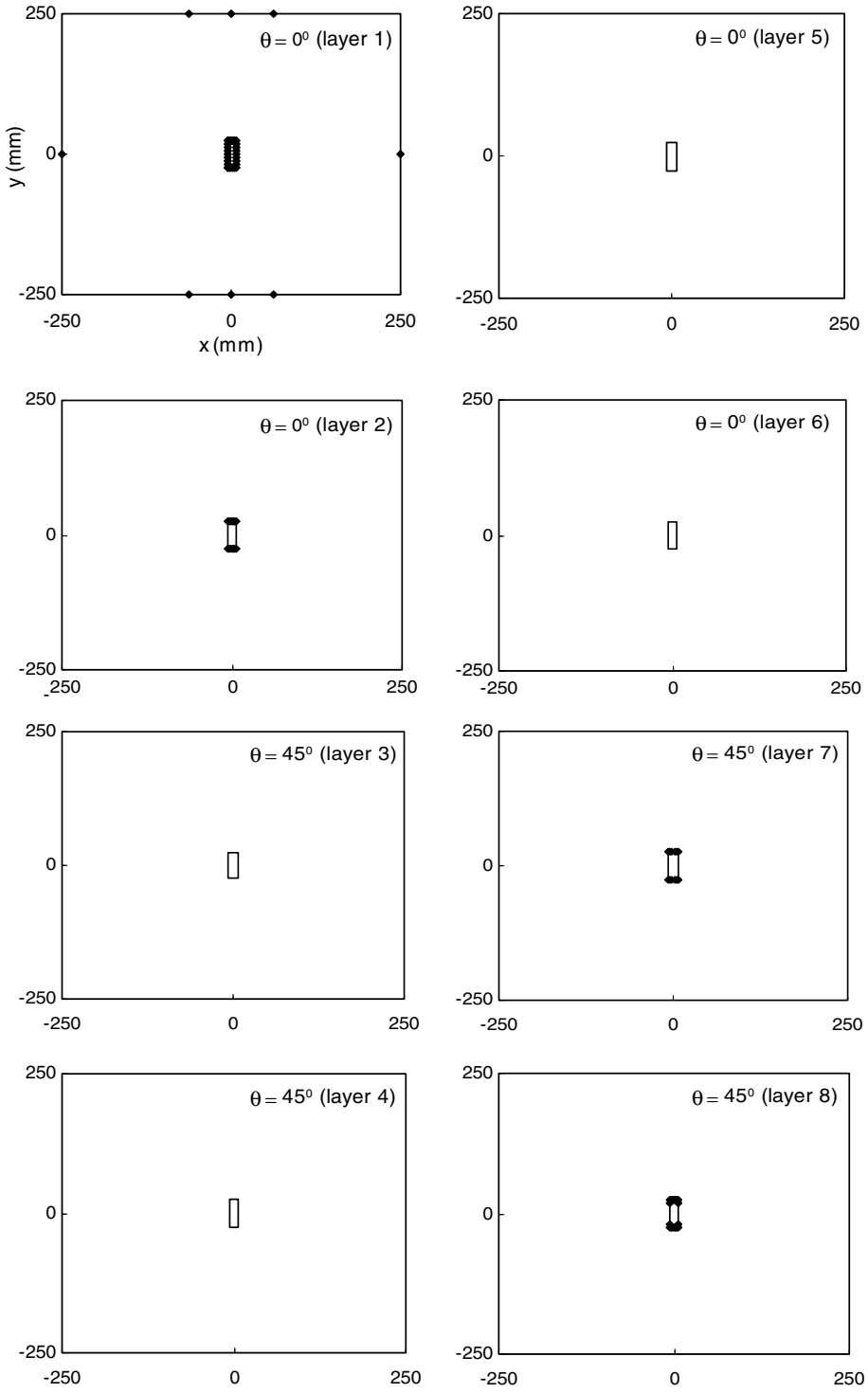

Fig. 12. Nodes in plastic region at each layer for antisymmetric ($[0°/45°]_2$) clamped supported laminated plates and 100 load steps.

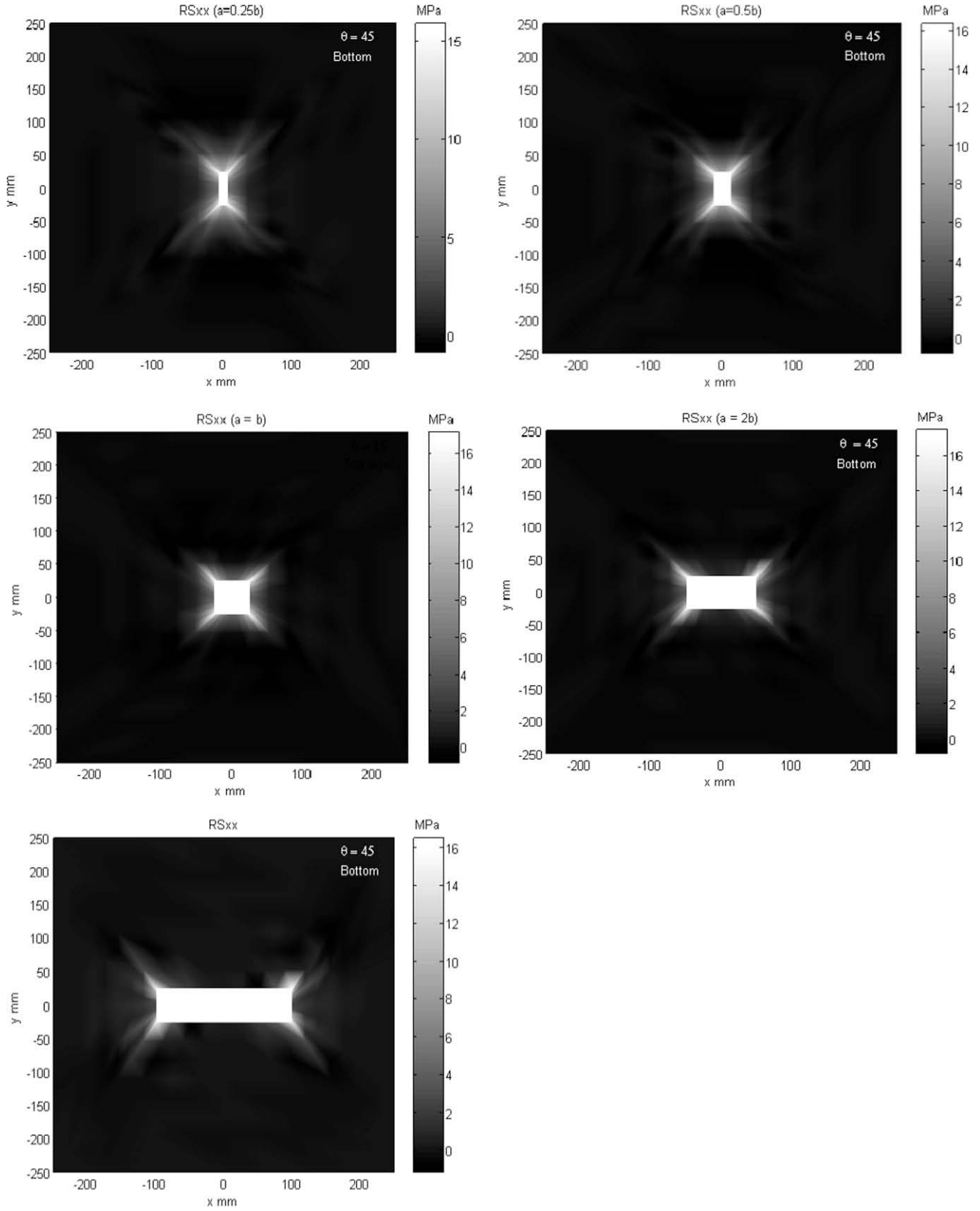

Fig. 13. Mapping of residual stress on the lower surface ($\theta = 45°$) for antisymmetric simply supported laminated plate ($[0°/45°]_2$) and different hole dimensions (a and b) (100 load steps).

due to woven reinforcement and loading conditions for symmetric and antisymmetric lamination. However these values at other angles layers (upper and lower surfaces) are different. This event is also the same in case of simply supported one. The σ_{xx},σ_{yy}, τ_{xy} elastic and RS_{xx}, RS_{yy}, RS_{xy} residual stress components are higher than the other components (τ_{xz}, τ_{yz}, RS_{xz}, RS_{yz}) because of the uniform

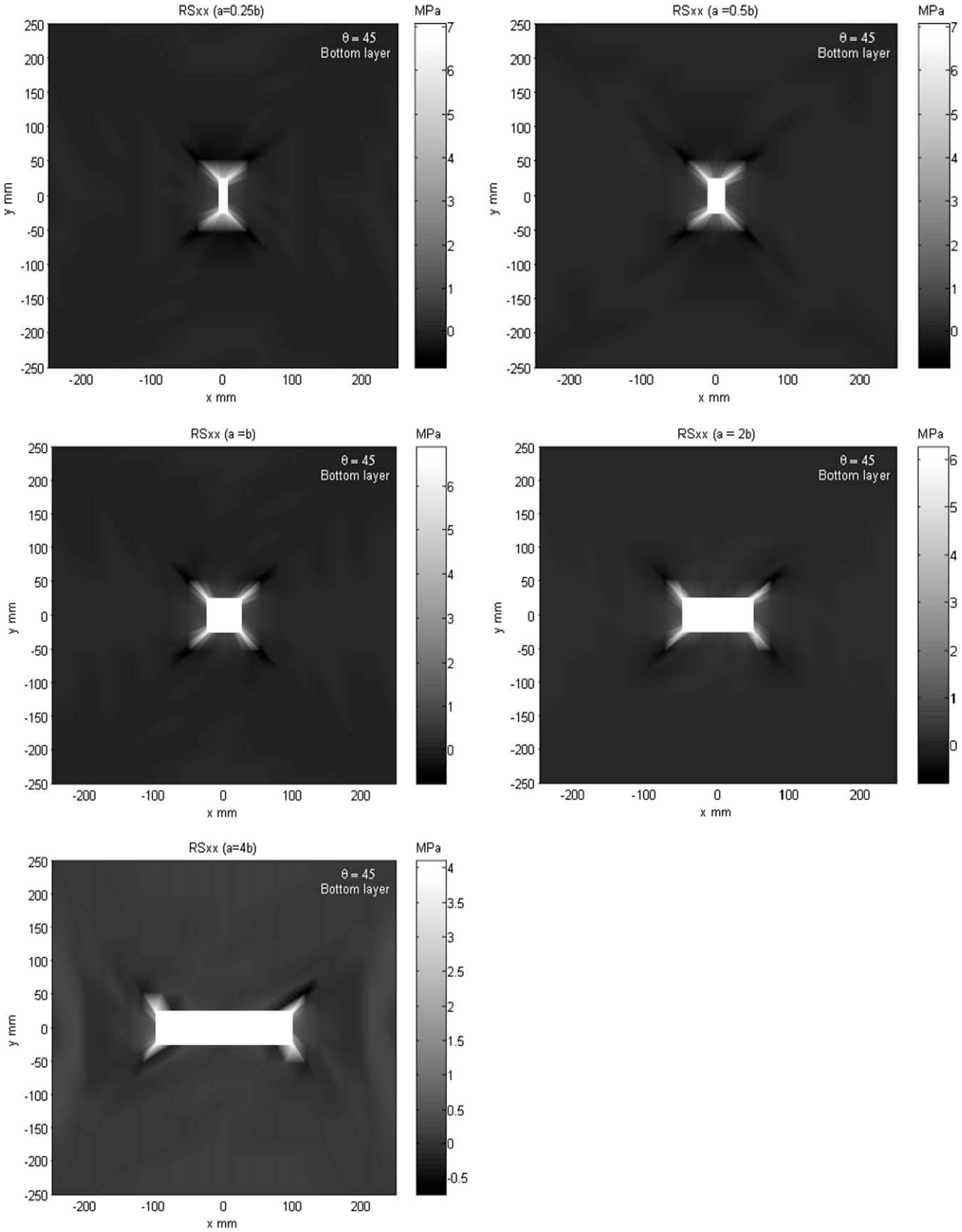

Fig. 14. Mapping of residual stress on the lower surface ($\theta = 45°$) for antisymmetric clamped laminated plate ($[0°/45°]_2$) and different hole dimensions (a and b) (100 load steps).

transverse load. The elastic and residual stress values at upper and lower surfaces reinforced in $\theta = 45°$ are lesser than those in other angles for symmetric and antisymmetric lamination clamped case.

Table 7 produces the maximum stresses in simply supported case for $[0°/\theta°]_2$ and symmetric and antisymmetric lamination. The results in Table 7 are some differences given in Table 6. Firstly,

the chosen constant uniform load is 0.01079 MPa in simply supported case, since the selected value of constant uniform load is appropriate for observing yield point. The elastic and residual stress values in simply supported laminated plates are higher than those in clamped plates under the same loading conditions for all stacking sequences $[0°/\theta°]_2$. The calculated stress values at [0°/30°]–[0°/60°] and [0°/15°]–[0°/75°] stacking sequences are almost the same for clamped and simply supported cases because of woven fiber reinforcement.

The plotting of the residual stress components (RS_{xx}, RS_{yy}, RS_{xy}) on the top and bottom layers in the antisymmetric simply supported laminated plate ([0°/45°]) for 100 load steps (Figs. 7 and 8). As observed from these figures, the concentration of the stress takes place around the rectangular hole in the direction of the steel fibers due to the stress concentration. The highest values of RS_{xx} and RS_{yy} in layers of $\theta = 0°$ (top layer) have been obtained along the hole sides which are parallel to the x and y axes, respectively. Maximum RS_{xx} and RS_{yy} values in layers of $\theta = 45°$ (bottom layer) have been found in the direction of the reinforcement or at the corners because the fiber reinforcement is woven. The maximum RS_{xy} shear residual stress components on the upper and lower surfaces are obtained at the corners since the fibers on the lower surfaces are oriented in 45° from the x-axis. Because this direction is principal direction for shear stresses, the results were confirmed by other research [4].

The plotting of residual stress components for clamped case ($[0°/45°]_2$) is provided in Figs. 9 and 10, for 100 load steps. As noticed from these figures, the concentration of the residual stresses is obtained around the rectangular hole in the direction of the steel fibers for top layer ($\theta = 0°$). Occasionally, the concentration of the residual stresses take parts along the clamped sides (close the middle of the clamped sides) of the plate and partly around the hole with respect to the plate and the hole dimensions and load steps. This condition can be also noted in the literature [4]. The highest RS_{xx} and RS_{yy} values are found at the all corners of the hole in the direction of the reinforcement for bottom layer ($\theta = 45°$), as simply supported case. RS_{xy} values are compatible to those of simply ones. It should be expected that it is seen that the residual stress values for simply supported case higher than those for clamped case when the Figs. 7–10 are compared [4].

The distributions of the plastic region at each layer of the antisymmetric ($[0°/45°]_2$) simply supported and clamped laminated plates are presented in Figs. 11 and 12, respectively. The plastic regions take place around the hole of the plate for each layer. These regions tended to sway towards reinforcement direction. The largest plastic regions appear at the top and bottom layers (layer 1 and layer 8). The plastic regions or nodes number under yielding narrow at the layers (layer 3,6) which are the adjacent to the midplane due to the transversely loading condition. There is no yielding at the 4th and 5th layers. It is obviously observed that the highest residual stresses are obtained at the top and bottom layers. This result was concluded with agreement of the literature [4].

The variations of the plotting of the RS_{xx} with hole dimensions are obtained for θ=45° as observed from Figs. 13 and 14 for $[0°/45°]_2$. The concentration of the stresses occurs at the all of the corners due to the woven reinforcement and $\theta = 45°$ laminations for either simply supported or clamped cases. This condition is conclusive for all hole dimensions. The RS_{xx} values for different hole dimensions are nearly equal despite the yield points reduce with increasing hole dimension "a" (in Fig. 1) when the hole dimension "b" is constant. It must be taken into consideration that the load steps are constant as 100 after yielding for all hole dimensions. On this occasion, the variations of the RS_{xx} with respect to the hole dimension is almost the same for both of antisymmetric clamped and simply supported plates on lower surfaces.

The plastic zone formation around the rectangular hole expands as the number of iteration (25, 50, 75 and 100) raises for simply supported plates; the result is presented in Fig. 15. It expands parallel to the hole sides at the plate's upper surface ($\theta = 0°$), on the other hand this expansion occurs through the plate's diagonal at the lower surface. The clamped supported plate's plastic region expansion with respect to iteration number (25, 50, 75 and 100) is demonstrated in Fig. 16. In this condition, plastic region formation occurs at the plate's upper ($\theta = 0°$) and lower ($\theta = 45°$) surfaces only around the hole sides. However the plastic region formation has been observed at the plate's side which is parallel to the short side of the rectangular hole at the upper surface for 100 iterations.

The variations of yield points with different rectangular hole dimensions, (a and b), obtained for the $[0°/45°]_2$, $[45°/-45°]_2$, $[0°/30°]_2$, and $[30°/-30°]_2$ stacking sequences and simply supported antisymmetric and symmetric lamination are shown in Fig. 17. The magnitudes of yield points decrease with increasing short side (a) of rectangular hole. For a = 12.5 mm and b = 50 mm values considered, the $[0°/45°]_2$ and $[45°/45°]_2$ laminates antisymmetric laminations have the magnitudes of the yield points 0.0089 and 0.01169 MPa, respectively. But, for a = 200 mm and b = 50 mm values, the magnitudes of the yield points 0.0068 and 0.0068 MPa, respectively. Similar trend is observed for simply supported and symmetric lamination.

Fig. 18 shows the variations of yield points with different rectangular hole dimensions (a and b) for the stacking sequences ($[0°/45°]_2$–$[45°/45°]_2$) and clamped supported antisymmetric and symmetric lamination. Similarly, the yield point decreases while enlarge to (a) side of hole in both lamination. However, the yield point increases for the dimension of a = 200 and b = 50 mm rectangular hole.

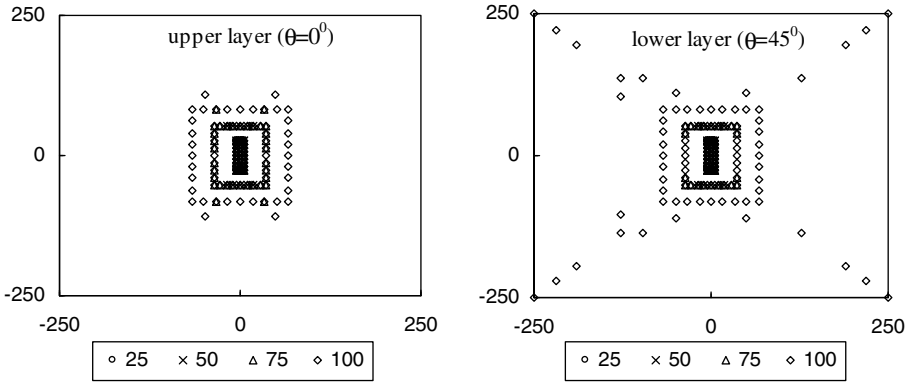

Fig. 15. Variations of plastic zones with load steps (iteration numbers) for simply supported plates ([0°/45°]) and antisymmetric lamination.

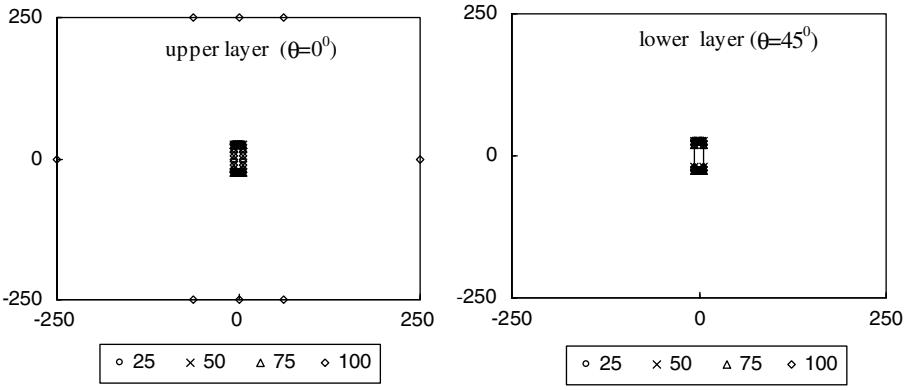

Fig. 16. Variations of plastic zones with load steps (iteration numbers) for clamped plates ([0°/45°]) and antisymmetric lamination.

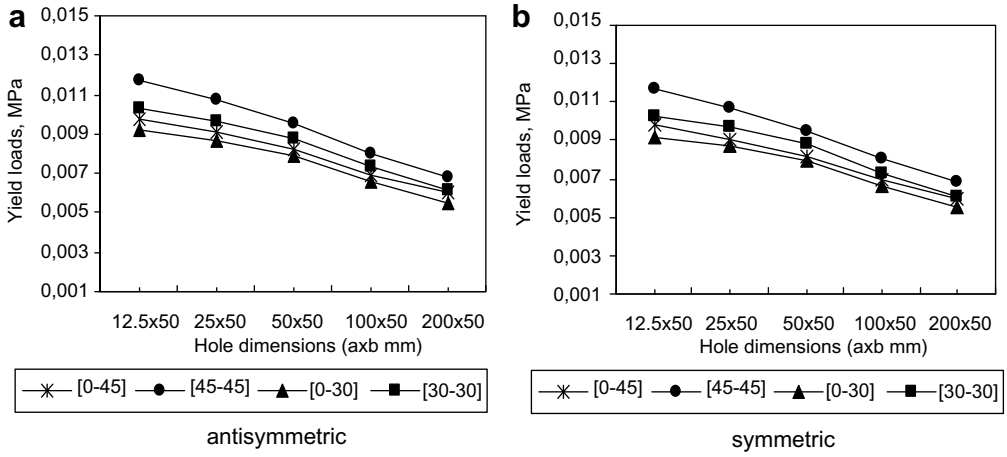

Fig. 17. Yield points with different hole dimensions (a and b) and different stacking sequences for simply supported lamination.

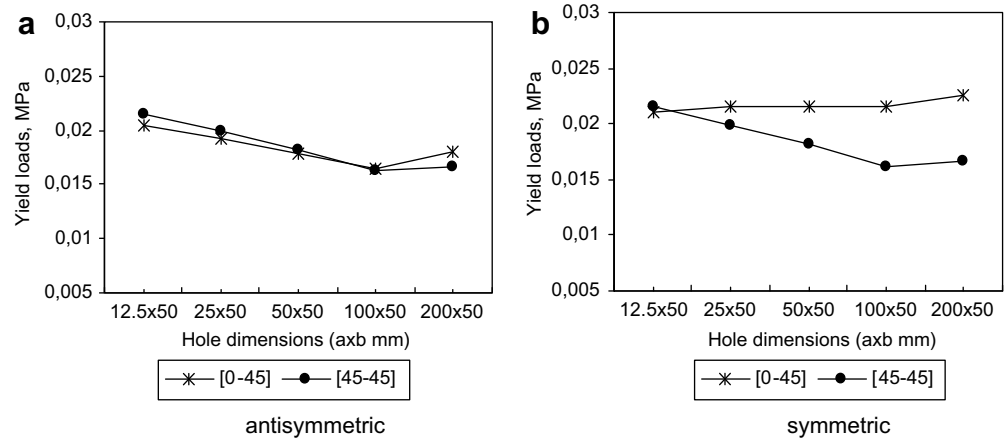

Fig. 18. Yield points with different hole dimensions (a and b) and different stacking sequences for clamped supported lamination.

3.1. Confirmation of the Analysis

Various analytical solutions have been reported by Karakuzu et al. [5], Sayman and Aksoy [14], Atas and Sayman [32] and it was considered to check the efficiency of the computer programs developed in this study. Karakuzu et al. examined elastic–plastic behaviour of woven-steel-fiber-reinforced thermoplastic laminated plates under in-plane loading [5]. Elastic–plastic stress analysis of simply supported and clamped aluminum metal-matrix laminated plates with a hole was determined by Sayman and Aksoy [14]. Atas and Sayman [32] worked elastic–plastic stress analysis and the expansion of the plastic zone in clamped and simply sup-

ported aluminum metal matrix laminated plates by FEM and experimental techniques (strain-gage).

4. Conclusions

The present study demonstrates the stress components and the expansion of the plastic region for the symmetric and antisymmetric simply supported and clamped laminated plates with rectangular hole under uniform static transverse loading. The influences of the reinforcement angle on the residual stresses and the plastic zones are achieved in woven-fiber reinforced thermoplastic composite laminated plates. The concluded results can be as below:

The stress concentrations can be increased through the residual stresses. Thus the failure of the laminated plate may be delayed and the load capacity of the plate increases by the residual stresses.

- The transverse uniform load values starting the yield have different value in small deformation limits for different stacking sequences.
- The yield points of the symmetric stacked plates are higher than those of antisymmetric stacked plates at $[0°/15°]_2$, $[0°/30°]_2$, $[0°/45°]_2$, $[0°/60°]$ and $[0°/75°]_2$ stacking sequences for clamped case.
- The yield points of either the symmetric or the antisymmetric laminated clamped plates are higher than those of simply supported plates.
- The residual stress values for simply supported case are higher than those for clamped case.
- The yield points of the clamped plates are higher than those of simply supported plates.
- The plastic regions expand away from the midplane. The largest regions are obtained at the top and bottom surfaces. In addition to this, the maximum elastic, and residual stress components are also obtained at the top and bottom surfaces for both boundary cases, simply supported and clamped cases.
- The plastic regions are revealed in or around the places where the biggest residual stresses occurred. There is a harmony with the relevant literature [2].
- The plastic regions expand in both symmetric and antisymmetric laminated plates in the direction of fibers around the square hole and the supports for both boundary cases.
- The elastic and residual stress values, reinforced in $\theta = 45°$ are smaller than the others orientation angles for antisymmetric lamination and both boundary cases at lower surfaces for both cases.
- For all stacking sequences, the stress values increase, furthermore, the plastic flow regions expand at either the relevant layers or the inner layers with increasing the load steps for both boundary cases.
- When the applied load is increased the plastic regions expand as the number of the yielding nodes increase. This behavior is obtained for all orientation angles in the simply supported and clamped laminated plates.
- The magnitudes of yield points increase with increasing hole dimensions due to the transverse loading condition.

References

[1] W.R. Yu, F. Pourboghrata, K. Chungb, M. Zampalonia, T.J. Kangb, Composite: Part A 33 (2002) 1095–1105.
[2] N. Arslan, M. Celik, N. Arslan, Compos. Struct. 55 (2002) 37–49.
[3] J.E. Shigley, Mechanical Engineering Design, first metric ed., McGraw-Hill, New York, 1986.
[4] N. Arslan, N. Arslan, F. Okumus, Compos. Sci. Technol. 64 (2004) 1147–1166.
[5] R. Karakuzu, C. Atas, H. Akbulut, Compos. Sci. Technol. 61 (2001) 1475–1483.
[6] A.P. Suvorov, G.J. Dvorak, Int. J. Solids Struct. 42 (2005) 2323–2344.
[7] G. Portu, L. Micele, S. Guicciardi, S. Fujimura, G. Pezzotti, Y. Sekiguchi, Compos. Sci. Technol. 65 (2005) 1501–1506.
[8] V.P.W. Shim, L.M. Yang, Int. J. Mech. Sci. 47 (2005) 647–665.
[9] O. Sayman, Composites: Part B 36 (2005) 61–72.
[10] N. Arslan, T. Özben, J. Reinf. Plast. Compos. 24 (2005) 5 457–469.
[11] R. Karakuzu, Z. Aslan, B. Okutan, Compos. Sci. Technol. 64 (2004) 1049–1056.
[12] N. Arslan, J. Reinf. Plast. Compos. 19 (17) (2000) 1389–1404.
[13] N.B. Bektaş, O. Sayman, Compos. Sci. Technol. 61 (2001) 1695–1701.
[14] O. Sayman, S. Aksoy, Compos. Struct. 53 (2001) 355–364.
[15] F. Okumus, J. Reinf. Plast. Compos. 24 (5) (2005) 471–484.
[16] O. Sayman, N. Arslan, H. Pıhtılı, J. Thermoplast. Compos. 6 (14) (2001) 523–538.
[17] A. Yapici, Ö.S. Şahin, M. Uyaner, J. Reinf. Plast. Compos. 24 (5) (2005) 503–511.
[18] F. Dubois, R. Keunings, Compos. Sci. Technol. 57 (1997) 437–450.
[19] S.Y. Hsu, T.J. Vogler, S. Kyriakides, Int. J. Plast. 15 (1999) 807–836.
[20] F.R. Gibson, Principles of Composite Material Mechanics, McGraw-Hill, International Editions, New York, 1994.
[21] C.T. Herakovich, Mechanics of Fibrous Composites, JohnWiley & Sons, Inc., New York, 1998.
[22] J.N. Reddy, An Introduction to the Finite Element Method, McGraw-Hill, Inc., Singapore, 1993.
[23] C.C. Lin, C.S. Kuo, J. Compos. Mater. 23 (1989) 536–553.
[24] K.J. Bathe, Finite Element Procedures in Engineering Analysis, Prentice-Hall Inc., Englewood Cliffs, New Jersey, 1982.
[25] E. Hinton, Introduction to Nonlinear Finite Element Analysis, NAFEMS, Bell and Bain Ltd., Glasgow, 1992.
[26] W. Johnson, P.B. Mellor, Engineering Plasticity, JohnWiley & Sons, New York, 1983.
[27] I.H. Tavman, J. Appl. Polym. Sci. 62 (1996) 2161–2167.
[28] R. Karakuzu, A. Özel, O. Sayman, Compos. Struct. 63 (3) (1996) 551–558.
[29] O. Sayman, M. Kayrici, Compos. Sci. Technol. 60 (2000) 623–631.
[30] G.A. Mohr, Finite Elements for Solids Fluids and Optimization, Oxford University Press, Oxford, 1992.
[31] N. Arslan, M.O. Kaman, M. Duranay, J. Reinf. Plast. Compos. 23 (18) (2004) 2025–2045.
[32] C. Atas, O. Sayman, Compos. Struct. 49 (2000) 9–19.
[33] Y.A. Bahei-El-Din, G.J. Dvorak, Trans. ASME 49 (1982) 740–746.
[34] D. Jegley, J. Compos. Mater. 27 (5) (1993) 526–538.
[35] H. Yıldız, O. Sayman, M. Aktaş, J. Reinf. Plast. Compos. 23 (18) (2004) 2065–2080.